Inorganic Chemistry

pubs.acs.org/IC

Article

Metal Flux Growth of Lanthanide Carbide Hydrides Using Anthracene

James T. Larson, Katelyn D. Wix, Banghao Chen, and Susan E. Latturner*

Cite This: *Inorg. Chem.* 2023, 62, 13277−13283

Read Online

ACCESS | Metrics & More | Article Recommendations | Supporting Information

ABSTRACT: Reactions of anthracene in Ln/T eutectic mixtures (Ln = La, Yb; T = Ni, Cu) have produced crystals of new complex lanthanide carbide hydride phases. The thermal decomposition of anthracene provides a source of both carbon and hydrogen. $LaCH_x$ forms in space group *Pnma* with unit cell parameters a = 7.2736(4) Å, b = 3.7218(2) Å, and c = 13.0727(7) Å. Yb_2CH_x forms in space group *P*-3*m*1 with unit cell parameters a = 3.5659(4) Å and c = 5.8000(8) Å, with a structure related to that of Ho_2CF_2. The presence of hydride in interstitial sites is supported by the formation of different compounds in the absence of hydrogen and by comparison to known hydride structures. ^{1}H nuclear magnetic resonance (NMR) spectra collected on $LaCH_x$ show two unique hydride resonances, in agreement with the two available interstitial sites. Density of states calculations show that filling the tetrahedral sites in $LaCH_x$ with hydrogen increases metallic behavior, while adding hydrogen into the tetrahedral sites in Yb_2CH_x induces the formation of a band gap.

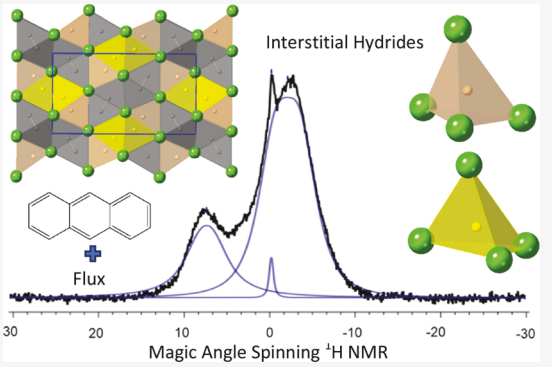

INTRODUCTION

Metal flux reactions make use of a low-melting metal or metal mixture as a solvent for the growth of intermetallic compounds. Unlike traditional solid-state methods, metal flux synthesis allows for lower reaction temperatures, with the reaction starting as soon as the reactants dissolve in the molten flux. Due to the lower temperatures, the likelihood of obtaining kinetically favorable products increases. Another useful quality of metal flux synthesis is that it is a solution method which provides a good environment for crystal growth, often yielding large, high-quality crystals for SCXRD and magnetic studies. Metal flux synthesis has been demonstrated to be an effective method for making rare earth intermetallics such as RNi_2Ge_2 (R = Y, La-Nd, Sm-Lu), $Pr_{26}Fe_{19}C_{29}$, and $Ce_{21}Fe_8Bi_7C_{12}$.[1−3]

Eutectic mixtures can be used as fluxes and are particularly useful in providing low-temperature lanthanide-rich growth media. Lanthanide elements themselves have melting points too high to be useful as fluxes. But early lanthanides (La, Ce, Pr, Nd) and ytterbium combine with late first-row transition metals to form low-melting eutectic mixtures. The fluxes explored in this work include La/Ni (75:25 mol %, mp 573 °C) and Yb/Cu (75:25 mol %, mp 472 °C). The La/Ni eutectic has been previously used to synthesize compounds including $La_{21}Fe_8M_7C_{12}$ (M = Sn, Bi, Sb, Te, Ge), $La_{15}(FeC_6)_4H$, and $La_{15}(FeC_6)_4F_2$.[3−5] It is particularly notable that these Ln/T fluxes are fruitful growth media for complex lanthanide carbides.

In this work, we have explored the use of anthracene ($C_{14}H_{10}$) as a carbon source in Ln/T flux reactions. We report two new lanthanide carbide structures: "LaC" and "Yb_2C". These grow as large metallic crystals with structures that differ from the previously reported binary lanthanide carbides. Because anthracene was used as a reactant, it is likely that these new structures are stabilized by hydrogen incorporation; we confirm that the same products do not form when carbon alone is used. Anthracene has acted as a source of both carbon and hydrogen in previous work, generating hydrogen interstitials in $La_{15}(C_6Fe)_4H$ and $Ce_4B_2C_2H_{2.42}$ confirmed by neutron diffraction.[4,6] While the presence of hydrogen has not been confirmed in the compounds reported here, it is likely that they are lanthanide carbide hydrides and are therefore referred to as $LaCH_x$ and Yb_2CH_x.

EXPERIMENTAL PROCEDURES

Warning: Pressure may be generated in the reaction ampule when the organic compound decomposes at high temperature. Small amounts of $C_{14}H_{10}$ should be used so that the pressure of gaseous decomposition products does not exceed 4 atm at maximum temperature. Suitable PPE (gloves and face shields) was used when removing the ampules from the furnace, and they were wrapped in an aluminum foil barrier before breaking them open in a fume hood.

Synthesis. The La/Ni eutectic mixture was made by arc melting appropriate amounts of each element together, using lanthanum

Received: May 9, 2023
Published: August 7, 2023

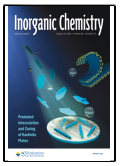

https://doi.org/10.1021/acs.inorgchem.3c01511
Inorg. Chem. 2023, 62, 13277−13283

pieces stored under mineral oil (Beantown Chemical, 99.9%) and nickel slugs (Beantown Chemical, 99.95%). Before arc melting, the lanthanum pieces were washed with hexanes to remove the mineral oil. Pellets of 75:25 mol % La/Ni were made by arc melting the appropriate masses of metals together under argon (purified by melting a Zr getter), flipping over the pellet and remelting 2−3 times, to insure homogeneity. The pellets were then broken into smaller pieces to be used in subsequent flux reactions. The flux pellets and all products grown in them are air-sensitive and must be stored under nitrogen or argon.

$LaCH_x$ was made by reacting 1.5 g of La/Ni flux with 0.2 mmol of anthracene ($C_{14}H_{10}$, Sigma-Aldrich, 97%). Anthracene was placed in an alumina crucible, followed by the flux. The crucible was placed in a silica sleeve with a wad of fiberfrax placed above the crucible. The sleeve was chilled in ice water before attaching it to a vacuum line. It was then flame-sealed under vacuum, and this ampule was placed into a programmable furnace. The reaction ampule was heated to 950 °C in 3 h and held there for 12 h. It was then cooled to 600 °C over the course of 120 h and left to anneal at 600 °C for 84 h at which point it was taken out of the furnace and centrifuged to separate the flux from the products. The resulting crystals are silver and rod-shaped with dimensions of ∼2 mm long and 0.25 mm wide, forming in clusters with high yield. They are very air-sensitive and must be stored in an inert atmosphere. Decomposition of crystals usually begins after ∼10 to 15 min in air. Elemental analysis was carried out using X-ray fluorescence (XRF) spectroscopy using a Panalytical Epsilon 3 X-ray fluorometer. A sample of 75 mg of $LaCH_x$ crystals were dissolved in 1 mL of 2 M HNO_3 (aq). This occurred with obvious effervescence, presumably from the formation of H_2 and CH_4 gases. The resulting solution was placed into a sample holder for data collection. The XRF spectrum (Figure S1) indicated the presence of lanthanum and only trace amounts of nickel (due to the La/Ni flux residue on the product surface).

Yb_2CH_x was made by reacting 7.76 mmol of Yb and 2.45 mmol of Cu powder (Alfa Aesar, 99.5%) with 0.1429 mmol of anthracene. Anthracene was placed in the bottom of the alumina crucible followed by Cu, with the Yb being placed on top of the other reactants. Yb will melt first at 819 °C, melting down onto the Cu, forming a 76:24 mol % eutectic mixture with a melting point of ∼500 °C. The ampule was flame-sealed and heated as described above; it was then removed from the oven at 600 °C and centrifuged. The crystals formed as silver, square-shaped plates with sides of ∼1 mm and widths less than 0.1 mm; the yield of this phase was very low (precluding analysis beyond single-crystal diffraction), and significant amounts of $YbCu_2$ by-products were present. Like $LaCH_x$, Yb_2CH_x is also air-sensitive and must be stored in an inert atmosphere.

Reactions were explored using 2 mmol carbon (acetylene carbon black, Strem Chemicals, 99.99%) in each of the Ln/T fluxes, with the same preparation and heating profile. These reactions yielded powders and crystals of previously reported binary carbides (see the Results and Discussion section).

Single-Crystal X-ray Diffraction. Suitable single crystals were mounted onto cryoloops using Parabar oil. Diffraction data were collected on a Rigaku XtaLAB Synergy-S diffractometer equipped with a HyPix-6000HE Hybrid Photon Counting (HPC) detector and Mo/Cu microfocus sealed X-ray sources. Measurements were taken at room temperature using Mo Kα radiation (λ = 0.71073 Å). CrysalisPro was used to integrate the datasets, and Shelxle was used to refine the structure.[7,8] The lanthanide atoms were located using direct methods, while least-squares refinement and difference Fourier maps were used to locate the position of carbon atoms. Hydrogen was placed in the two possible interstitial positions of $LaCH_x$ after optimizing the coordination environments and ensuring that associated Ln−H distances were in the range of those previously reported for lanthanide hydride compounds. Yb_2CH_x can be solved in both $P32_1$ and $P\bar{3}m1$; the latter was chosen because of its higher symmetry (#164) as well as it being the same space group as isostructural Ho_2CF_2. In Yb_2CH_x, hydrogen was placed in the tetrahedral interstitial site after it was chosen as the most likely position for hydrogen incorporation (see the Results and Discussion section). The carbon atoms were refined isotropically. Crystallographic data and collection parameters are shown in Table 1; additional information can be found as CIF files (CCDC deposition numbers 2260681 for $LaCH_x$ and 2261829 for Yb_2CH_x).

Table 1. Crystallographic Data and Collection Parameters for the Title Compounds

formula	$LaCH_x$	Yb_2CH_x
formula weight[a] (g/mol)	150.916	358.119
crystal system	orthorhombic	trigonal
space group	*Pnma*	$P\bar{3}m1$
a (Å)	7.2736(4)	3.5657(5)
b (Å)	3.7218(2)	
c (Å)	13.0727(7)	5.8008(8)
Z	8	1
volume (Å^3)	353.89(3)	63.87(2)
density, calc (g/cm^3)	5.703	9.362
index ranges	$-10 < h < 9$	$-4 < h < 3$
	$-5 < k < 4$	$-4< k < 4$
	$-16 < l < 17$	$-7 < l < 7$
reflections collected	5122	424
temperature (K)	296	298
radiation	Mo Kα	
unique data/parameters	568/25	82/5
θ values (deg)	min = 4.192	min = 3.512
	max = 30.890	max = 29.713
μ (mm^{-1})	23.538	72.353
R_1/wR_2 ($I > 2\sigma(I)$)	0.0276/0.0671	0.0473/0.1124
R_1/wR_2 (all data)	0.0299/0.0683	0.0481/0.1130
GoF	1.122	1.157
highest peak/hole (e$^-$/Å^3)	2.175/−1.969	4.212/−3.906

[a]Formula weight based on lanthanide and carbon only due to uncertainty about the hydrogen content.

Powder X-ray Diffraction. Powder X-ray diffraction was used to identify the powder products from reactions of Yb/Cu flux and carbon. The instrument used was a Rigaku SmartLab diffractometer equipped with a Cu Kα radiation source. $Yb_{15}C_{19}$ was identified along with unreacted carbon.

NMR Spectroscopy. Magic-angle spinning ^{1}H NMR studies of $LaCH_x$ were carried out on a Bruker AVIII HD 500 MHz WB spectrometer (B_0 = 11.7 T) with a ^{1}H Larmor frequency of 500.34 MHz. All sample preparation was performed in a glove box with an argon environment. Crystals of $LaCH_x$ were ground to a powder with KBr in a 2:3 volume ratio of $LaCH_x$/KBr to facilitate spinning. The resulting powder sample was packed into a 2.5 mm rotor. The sample was spun at 25 kHz. Data were collected after 1024 scans with a recycle delay of 5 s after optimization. The same empty rotor was measured under the same conditions prior to being packed with the sample to obtain a background measurement that was subtracted from the $LaCH_x$ spectra. Adamantane was used as a second-order reference at 1.75 ppm to TMS.

Electronic Structure Calculations. Density of states calculations (DOS) were performed using the Stuttgart TB-LMTO-ASA (tight binding-linear muffin tin orbital-atomic sphere approximation) program package.[9] Models were derived from single-crystal data, with interstitial sites assumed to be either completely empty or completely full. To avoid issues that arise from partially filled f-orbitals, ytterbium was modeled as lutetium. The La (6s, 5d, 4f), Lu (6s, 5d, 4f), C (2s, 2p), and H(1s) basis sets were used, with La (6p) and C (3d) being downfolded. The tetrahedron method was used to integrate over the Brillouin zone.[10]

https://doi.org/10.1021/acs.inorgchem.3c01511
Inorg. Chem. 2023, 62, 13277−13283

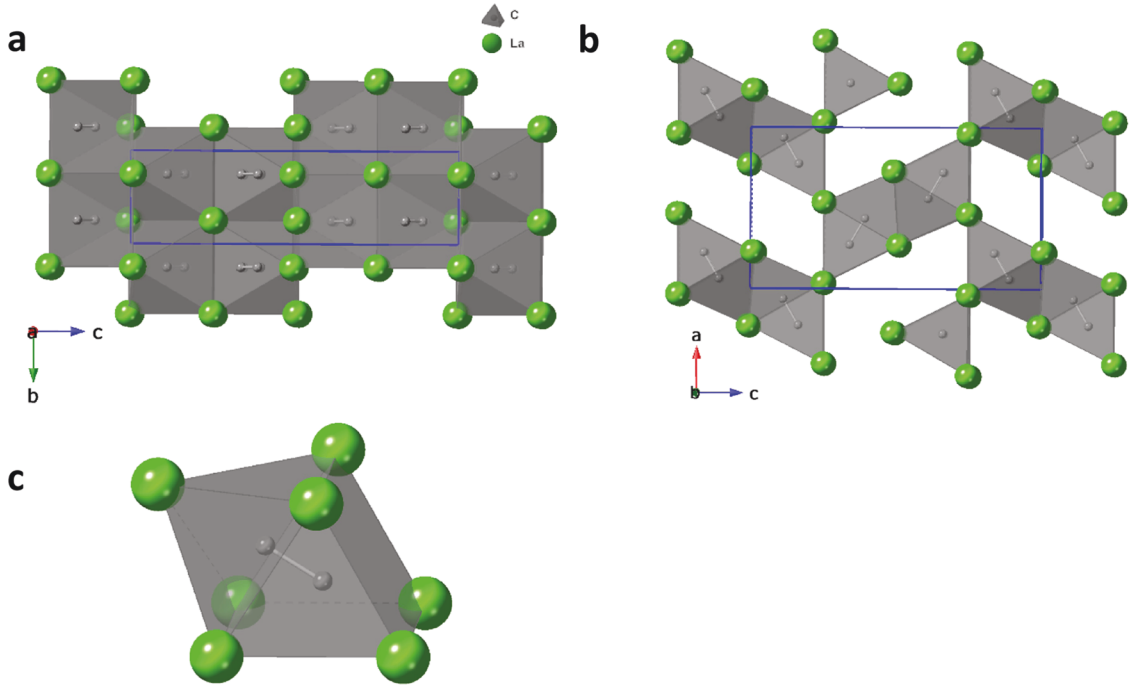

Figure 1. Structure of $LaCH_x$ shown in polyhedral mode. (a) View down the *a*-axis. (b) View down the *b*-axis. (c) Coordination environment of C_2 units in $LaCH_x$. The C_2 unit is coordinated to 7 La^{3+} atoms forming a monocapped trigonal prism.

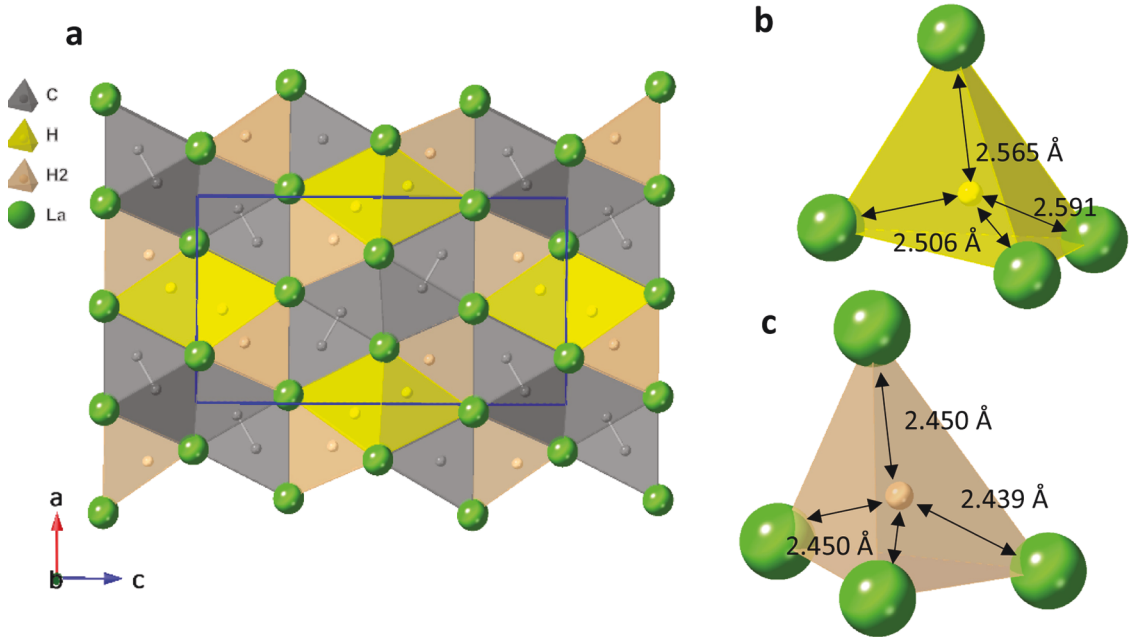

Figure 2. (a) Structure of $LaCH_x$ with possible hydride sites shown. (b) Larger 4*c* interstitial hydride site with La−H distances shown. (c) Smaller 4*c* hydride interstitial site with La−H distances shown.

RESULTS AND DISCUSSION

Synthesis. Gai et al. demonstrated that when anthracene is heated to 700 °C in an argon environment, it decomposes into propane and ethylene along with trace amounts of methane and hydrogen.[11] Recent work by McFarland showed that methane gas decomposes into solid carbon and hydrogen gas when bubbled through a molten bismuth/nickel alloy.[12] We are exploring thermal decomposition of anthracene as a source of gaseous species which will then dissolve in the molten flux to provide carbon and hydrogen to the reaction. Metal flux synthesis with anthracene has been demonstrated to produce intermetallic compounds containing carbon and interstitial hydride sites. Examples include $La_{15}(FeC_6)_4H$, $Ce_4BC_2H_{2.42}$, and $La_2BC_2H_{1.69}$.[4,6] All of these examples were grown from anthracene decomposition products interacting with other reactants (iron or boron) in Ln/T flux. We wanted to explore what occurs in the absence of other reactants, to see if Ln/T flux with anthracene alone would produce lanthanide carbides.

Yb_2CH_x was initially made by reacting anthracene with pre-arc-melted 75:25 mol % Yb/Cu flux. This reaction only yielded

https://doi.org/10.1021/acs.inorgchem.3c01511
Inorg. Chem. 2023, 62, 13277−13283

a few small crystals. In attempting to reproduce it, when the reaction was taken out of the furnace and centrifuged, the resulting product was a large chunk that looked as if the flux had already solidified. This occurred several times with different batches of pre-melted flux. It was observed that when arc melting the flux, black vapor was produced and would coat the inside of the arc melter chamber. Because Yb has a relatively low boiling point of 1,196 °C, it is thought that the black vapor is Yb vapor being lost, and the resulting pellet of flux has less Yb than intended and resulted in a higher melting point. Subsequent reactions were tried without pre-arc melting the flux, and these produced better yields.

Parallel reactions were carried out using carbon instead of anthracene, to observe the results if no source of hydrogen is present. Reactions of carbon in La/Ni eutectic yielded small, irregular cubic La_2C_3 crystals with diameters up to 0.25 mm. Reactions of carbon in Yb/Cu flux produced powdered $Yb_{15}C_{19}$. Since the Ln/T flux reactions with anthracene yielded different compounds with structures not previously reported in the literature, it is likely that these products are stabilized by interstitial hydride sites.

Structure of $LaCH_x$. $LaCH_x$ crystallizes with an orthorhombic structure in space group *Pnma* that is shown in Figure 1. It features layers of La atoms separated by C_2 units with C−C bond lengths of 1.36(1) Å. That is comparable to other C−C distances in rare earth compounds such as 1.284 Å in LaC_2 and 1.325 Å in $La_8(C_2)_4Cl_5$; these units are presumed to be double-bonded ethylenide units (C_2^{4-}), although these metallic phases are not charge-balanced.[13,14] The C_2 units in $LaCH_x$ are in an unusual coordination environment. Usually, C_2 units are octahedrally coordinated to 6 metal cations as is found in LaC_2, $La_8(C_2)_4Cl_5$, $Ca_5Cl_3(C_2)$(CBC), and $Ce_5B_2C_6$. However, in $LaCH_x$, the C_2 units are coordinated to 7 La^{3+} atoms in a monocapped trigonal prism.[13−16] To our knowledge, this environment for a C_2 unit is novel for rare earth carbide intermetallics. The La−C distances range from 2.497(7) to 2.892(6) Å. This is shorter than those found in other lanthanum carbides (2.648−2.857 Å in LaC_2 and 2.712−2.825 Å in La_2C_3), but a 2.302 Å La−C distance is reported in $La_4Cl_5C_2$.[13,17,18]

A possible location for hydrogen interstitials in $LaCH_x$ is on the 4*c* Wyckoff site shown in Figure 2b. This position places the hydrogen atom in tetrahedral coordination with La−H distances ranging from 2.51 to 2.57 Å. These distances closely resemble those found in the hydrogen tetrahedral site of LaH_2 (2.454 Å).[19] This tetrahedral interstitial site is also very similar to that seen in $La_3BC_2H_{1.69}$, which has La−H_{tet} bonds in the range of 2.47−2.54 Å. It is notable that this borocarbide compound has both tetrahedral and octahedral hydride interstitials, but neutron diffraction data confirmed that the tetrahedral sites are preferentially filled. For the compound reported here, placing hydrogen in this tetrahedral interstitial location gives a stoichiometry of La_2C_2H with $Z = 4$. There is another tetrahedral site available shown in Figure 2c. This site is smaller, with the La−H distances ranging from 2.44 to 2.45 Å. This distance is slightly shorter than those observed in LaH_2; however, it may still be possible for some hydrogen to incorporate into this site. If both possible hydride sites are occupied at the same time, the H−H distance would be too short, 1.38 Å, suggesting that if one site is occupied, then the other is not. The larger hydride site has a volume of 8.040 $Å^3$, while the smaller hydride site has a volume of 7.135 $Å^3$.

Solid-state ^1H MAS-NMR was performed on $LaCH_x$ to confirm the presence of hydrogen. As seen in Figure 3, there

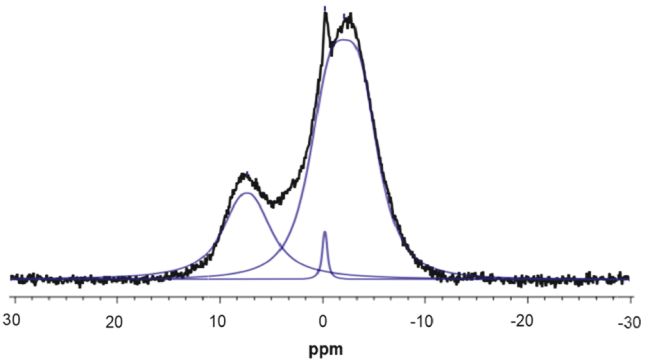

Figure 3. ^1H MAS-NMR spectrum of $LaCH_x$. The peak at 8.2 ppm is attributed to the smaller hydride site and the peak at −2.8 ppm is attributed to the larger hydride site. The peak at −0.5 ppm is due to surface hydroxides.

are three hydrogen resonances in the spectrum at 8.2, −0.5, and −2.8 ppm with an integration ratio of 10:1:35. The sharp peak at −0.5 ppm is attributed to surface hydroxide contamination due to this peak increasing in size relative to the other peaks when a sample of $LaCH_x$ that has been exposed to the atmosphere for about an hour is run. This leaves two distinct peaks, indicating that there are two crystallographically unique hydride sites in the structure. The peak at 8.2 ppm closely resembles that of BaH_2 with a shift of 8.7 ppm.[20] The shift for the −2.8 ppm peak is close to the −1.2 shift found in $LiBH_4$.[21] The peak at −2.8 ppm is 3.5 times as intense as the peak at 8.2 ppm, indicating that the hydrogen in that site is 3.5 times as abundant. It is assumed that the larger peak at −2.8 ppm is from the hydrogen in the larger tetrahedral site, while the smaller peak is from the hydrogen in the less favorable smaller tetrahedral site.

Structure of Yb_2CH_x. Yb_2CH_x crystallizes in the trigonal space group *P*-3*m*1 (see Figure 4). The ytterbium atoms are in the same positions as *hcp* Yb (high temperature allotrope;

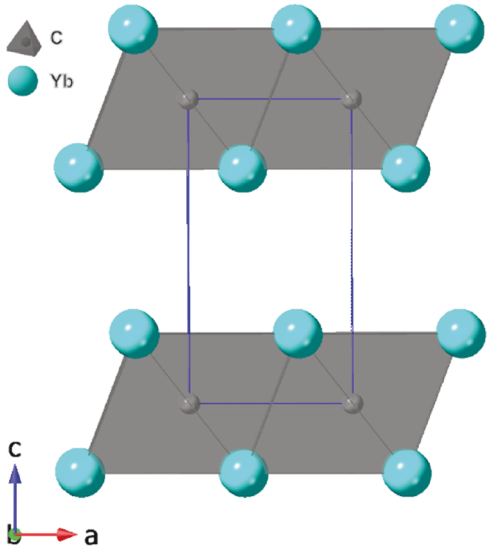

Figure 4. Structure of Yb_2CH_x shown in polyhedral mode, with hydride sites omitted. Carbon octahedral sites are shown in gray.

https://doi.org/10.1021/acs.inorgchem.3c01511
Inorg. Chem. 2023, 62, 13277−13283

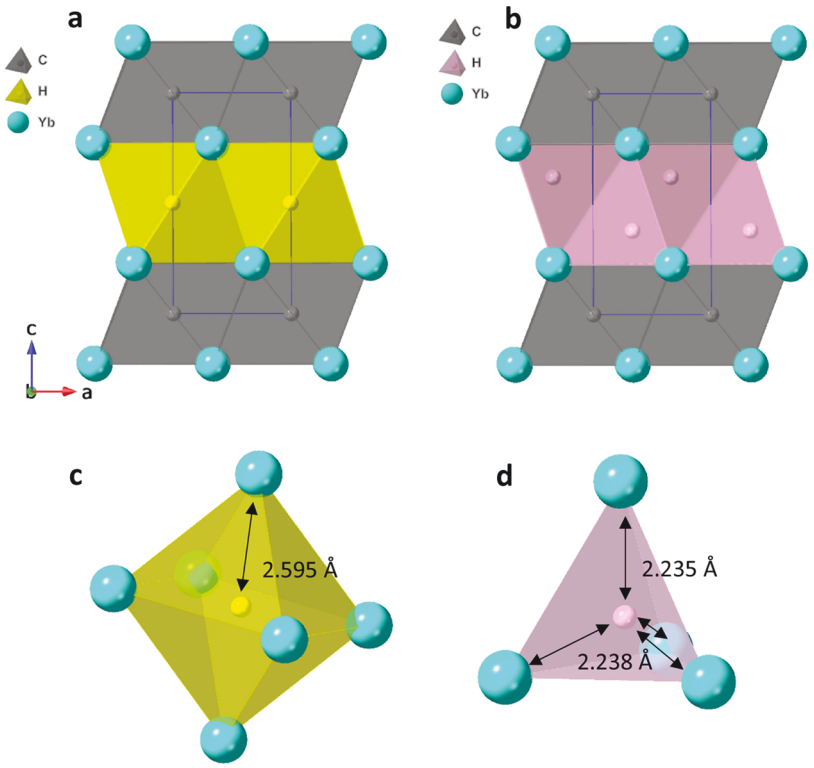

Figure 5. (a) Yb_2CH_x shown in polyhedral mode with an octahedral 1*b* site shown in yellow. (b) Yb_2CH_x shown in polyhedral mode with a tetrahedral 2*d* site shown in pink. (c) Octahedral 1*b* site with the Yb−H distance shown. (d) Tetrahedral 2*d* site with Yb−H distances shown.

space group *P*63/*mmc*), with added interstitial C atoms.[22] These single carbons are octahedrally coordinated to the surrounding Yb atoms with a distance of 2.5401(7) Å. This is comparable to the Yb−C distance of 2.404−2.647 Å found in YbC_2 (which has a C_2 unit in an octahedral site), as well as the Yb−C distance of 2.501 Å found in cubic Yb_2C (which has a single C atom in an octahedral site).[23,24] Counterintuitively, the addition of C reduces the Yb−Yb distances from 3.911 Å in *hcp* Yb to 3.61(2) Å in Yb_2CH_x. This is very similar to the Yb−Yb distance found in YbC_2 (3.63 Å).

There are two possible locations for a hydrogen interstitial site, shown in Figure 5. The first location for hydrogen would be on the 1*b* Wyckoff site octahedrally coordinated to the surrounding Yb atoms. This results in a H−Yb distance of 2.595 Å, which compares well to the 2.596 Å distance seen for the octahedral hydride site of YbH_3.[25] Placing hydrogen in this site gives a stoichiometry of Yb_2CH. Another possible location for a hydride site is at the 2*d* Wyckoff site. This is a tetrahedral interstitial site with H−Yb distances of 2.235−2.238 Å; its full occupancy yields a stoichiometry of Yb_2CH_2. These H−Yb distances are within the range found in the tetrahedral site of YbH_2 (2.14−2.37 Å).[26] It is possible for both interstitial sites to be occupied at the same time, yielding a stoichiometry of Yb_2CH_3. If both sites are filled, the 1*b* site and the 2*d* site will be 2.17 Å from each other. This distance is acceptable, as the minimum separation of hydride interstitial sites in intermetallics is 2.1 Å.[27] Neutron diffraction would be required to determine the siting and occupancy of hydrogen.

Support for the occupancy of the tetrahedral sites (Yb_2CH_2 model) comes from similarities to isostructural Ho_2CF_2, wherein fluorine is incorporated onto the 2*d* Wyckoff site.[28] It is also isostructural to $La_2SeD_{1.6}$; the presence (and partial occupancy) of deuterium in the tetrahedral 2*d* sites in that compound was confirmed by neutron diffraction.[29] It is therefore assumed that the hydride is located in tetrahedral interstitial sites. The unit cell parameters of Yb_2CH_2 are smaller than those reported for Ho_2CF_2, indicating that Yb is likely trivalent instead of divalent. The full occupancy of the tetrahedral site would therefore lead to charge-balancing, with charges formally assigned as $(Yb^{3+})_2(C^{4-})(H^-)_2$.

Electronic Structure Calculations. The calculated density of states (DOS) data for $LaCH_x$ is shown in Figure 6. Two structural models were used, one containing just the La and C observed with SCXRD, and a second with hydrogen added into both possible tetrahedral interstitial sites. In the LaC model, the Fermi level falls in a stabilizing pseudogap. The carbon states lie between −3.5 and −4.5 eV, with a large peak around −3.2 eV. The carbon states being below the Fermi level is in agreement with the anionic nature of the C_2 unit. In the $LaCH_2$ model with both interstitial sites filled, there is a much greater number of states at the Fermi level indicating increasing metallic behavior. The band of carbon states becomes broader, splitting the large peak at −3.2 eV. The hydrogen states form a band centered around −5 eV.

Figure 7 shows the DOS data for three models of Yb_2CH_x. Because Yb^{3+} has a partially filled f-orbital, Lu^{3+} was used in the calculations. The first model compound, Lu_2C, contains only the metal and carbon positions observed with SCXRD. The second model compound is Lu_2CH_3 (with both possible hydride interstitial sites filled), and the third model is Lu_2CH_2 (with the tetrahedral hydride sites filled and the octahedral sites empty). In all three models, the Lu^{3+} f-orbitals yield a sharp peak (located in the −3 to −5 eV range), in agreement with their filled and localized nature. The Lu_2C model has the carbon states located from −2.5 to −4.5 eV, while adding hydrogen moves them up to −0.5 to −2 eV in the Lu_2CH_3

https://doi.org/10.1021/acs.inorgchem.3c01511
Inorg. Chem. 2023, 62, 13277−13283

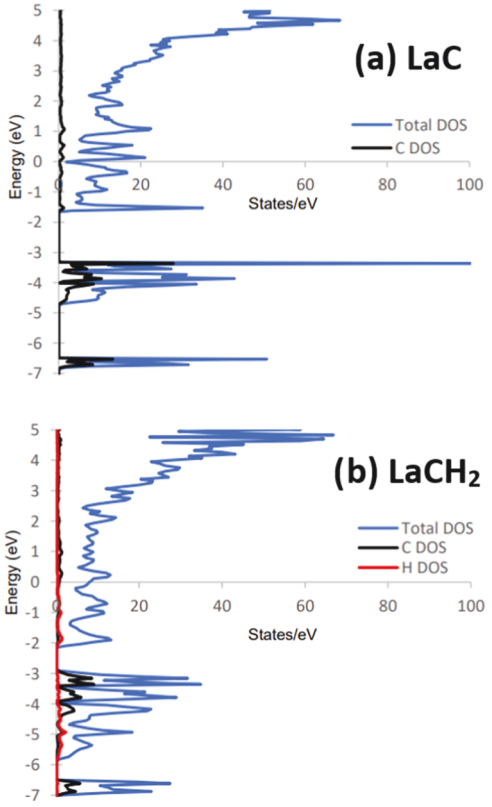

Figure 6. Density of states data for two model compounds of $LaCH_x$. (a) DOS plot for the LaC model. (b) DOS plot for $LaCH_2$, with both interstitial hydride sites filled.

model and −1 to −2 eV in the Lu_2CH_2 model. In the Lu_2CH_3 model, the hydrogen states are positioned in the range from −1 to −5 eV. In the Lu_2CH_2 model, the hydride states are more strongly localized, evidenced by the sharper peaks at −3.5 and −4 eV. More critically, the Lu_2C and Lu_2CH_3 compounds feature states at the Fermi level and are therefore metallic. On the other hand, Lu_2CH_2 has a small band gap of 0.2 eV indicating that this model is a semiconductor, in agreement with its charge-balanced nature. However, it is notable that the hydride sites in the isostructural $La_2SeH_{1.6}$ compound are partially occupied,[29] which may also be the case for Yb_2CH_2.

CONCLUSIONS

New lanthanide carbide hydrides have been synthesized by reacting Ln/T flux with anthracene. Both $LaCH_x$ and Yb_2CH_x compounds only grow in the presence of a hydrogen source, suggesting that incorporation of hydrogen is necessary for stabilizing the structures. ^{1}H MAS-NMR verified the presence of two hydrogen sites in $LaCH_x$ with the occupancy of one site being 2−3 times that of the other. Neutron diffraction would be required to verify the occupancy of these sites as well as confirm the presence of hydrogen in Yb_2CH_x. This work demonstrates a new method for obtaining novel rare earth hydrides that may lead to the discovery of new hydrogen storage materials or, if applied to synthesis of magnetic compounds, may lead to control of magnetic properties.

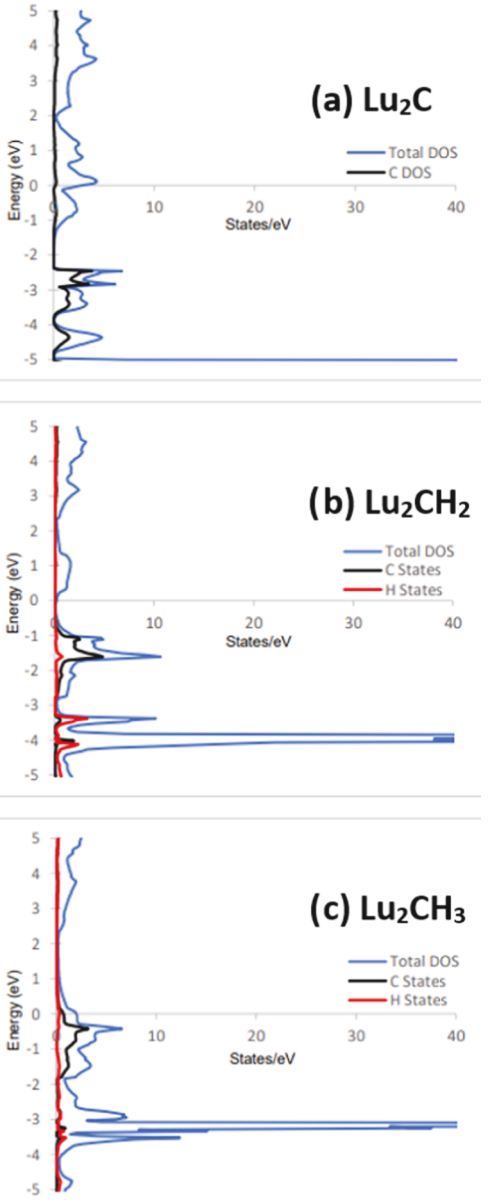

Figure 7. Density of states data for three model compounds of Yb_2CH_x. (a) DOS plot for the Lu_2C model. (b) DOS plot for the Lu_2CH_2 model. (c) DOS plot for the Lu_2CH_3 model.

ASSOCIATED CONTENT

Supporting Information

The Supporting Information is available free of charge at https://pubs.acs.org/doi/10.1021/acs.inorgchem.3c01511.

X-ray fluorescence (XRF) spectrum for solution of $LaCH_x$ dissolved in acid (Figure S1) (PDF)

Accession Codes

CCDC 2260681 and 2261829 contain the supplementary crystallographic data for this paper. These data can be obtained free of charge via www.ccdc.cam.ac.uk/data_request/cif, or by emailing data_request@ccdc.cam.ac.uk, or by contacting The Cambridge Crystallographic Data Centre, 12 Union Road, Cambridge CB2 1EZ, UK; fax: +44 1223 336033.

https://doi.org/10.1021/acs.inorgchem.3c01511
Inorg. Chem. 2023, 62, 13277−13283

AUTHOR INFORMATION

Corresponding Author

Susan E. Latturner − *Department of Chemistry and Biochemistry, Florida State University, Tallahassee, Florida 32306, United States;* orcid.org/0000-0002-6146-5333; Email: slatturner@fsu.edu

Authors

James T. Larson − *Department of Chemistry and Biochemistry, Florida State University, Tallahassee, Florida 32306, United States*

Katelyn D. Wix − *Department of Chemistry and Biochemistry, Florida State University, Tallahassee, Florida 32306, United States*

Banghao Chen − *Department of Chemistry and Biochemistry, Florida State University, Tallahassee, Florida 32306, United States*

Complete contact information is available at: https://pubs.acs.org/10.1021/acs.inorgchem.3c01511

Notes

The authors declare no competing financial interest.

ACKNOWLEDGMENTS

This research was supported by the Division of Materials Research of the National Science Foundation (DMR-21-26077). This work utilized the resources of the X-ray Characterization Center in the Department of Chemistry and Biochemistry at FSU (FSU075000XRAY).

REFERENCES

(1) Bud'ko, S. L.; Islam, Z.; Wiener, T. A.; Fisher, I. R.; Lacerda, A. H.; Canfield, P. C. Anisotropy and metamagnetism in the RNi2Ge2 (R = Y, La−Nd, Sm−Lu) series. *J. Magn. Magn. Mater.* **1999**, *205*, 53−78.

(2) Jayasinghe, A. S.; Latturner, S. E. Metal Flux Growth of Praseodymium Iron Carbides Featuring FeC3 Units. *Cryst. Growth Des.* **2021**, *21*, 103−111.

(3) Benbow, E. M.; Dalal, N. S.; Latturner, S. E. Spin Glass Behavior of Isolated, Geometrically Frustrated Tetrahedra of Iron Atoms in the Intermetallic La21Fe8Sn7C12. *J. Am. Chem. Soc.* **2009**, *131*, 3349−3354.

(4) Engstrand, T. O.; Cope, E. M.; Vasquez, G.; Haddock, J. W.; Hertz, M. B.; Wang, X.; Latturner, S. E. Flux Synthesis of a Metal Carbide Hydride Using Anthracene As a Reactant. *Inorg. Chem.* **2020**, *59*, 11651−11657.

(5) Larson, J. T.; Latturner, S. E. Flux Growth of an Intermetallic with Interstitial Fluorides via Decomposition of a Fluorocarbon. *Inorg. Chem.* **2023**, *62*, 1508−1512.

(6) Hertz, M. B.; Baumbach, R.; Wang, X.; Latturner, S. E. Unexpected Hydride: Ce4B2C2H2.42, a Stuffed Variant of the Nd2BC Structure Type. *Cryst. Growth Des.* **2021**, *21*, 5164−5171.

(7) *CrysAlisPRO*; Oxford Diffraction/Agilent Technologies UK Ltd.: Yarnton, England, 2014.

(8) Hübschle, C. B.; Sheldrick, G. M.; Dittrich, B. ShelXle: a Qt graphical user interface for SHELXL. *J. Appl. Crystallogr.* **2011**, *44*, 1281−1284.

(9) Tank, R.; Jepsen, O.; Burkhardt, A.; Andersen, O. The TB-LMTO-ASA Program, version 4.5, Stuttgart, Germany, 1994.

(10) Blöchl, P. E.; Jepsen, O.; Andersen, O. K. Improved tetrahedron method for Brillouin-zone integrations. *Phys. Rev. B* **1994**, *49*, 16223−16233.

(11) Gai, C.; Dong, Y.; Yang, S.; Zhang, Z.; Liang, J.; Li, J. Thermal decomposition kinetics of light polycyclic aromatic hydrocarbons as surrogate biomass tar. *RSC Adv.* **2016**, *6*, 83154−83162.

(12) Upham, D. C.; Agarwal, V.; Khechfe, A.; Snodgrass, Z. R.; Gordon, M. J.; Metiu, H.; McFarland, E. W. Catalytic molten metals for the direct conversion of methane to hydrogen and separable carbon. *Science* **2017**, *358*, 917−921.

(13) Babizhetskyy, V.; Jepsen, O.; Kremer, R. K.; Simon, A.; Ouladdiaf, B.; Stolovits, A. Structure and bonding of superconducting LaC2. *J. Phys.: Condens. Matter* **2014**, *26*, No. 025701.

(14) Mattausch, H.; Simon, A.; Kienle, L.; Köhler, J.; Hoch, C.; Nuss, J. Gewellt und eben − La6(C2)-Oktaederschichten in Lanthancarbidchloriden. *Z. Anorg. Allg. Chem.* **2008**, *634*, 2765−2776.

(15) Reckeweg, O.; Meyer, H.-J. Ca5Cl3(C2)(CBC): A Compound with a Layer Structure and an Unusual Anion Combination. *Angew. Chem., Int. Ed.* **1998**, *37*, 3407−3410.

(16) Bauer, J.; Bars, O. The crystal structure of the carbon-rich rare earth borocarbide Ce5B2C6. *J. Less Common Met.* **1982**, *83*, 17−27.

(17) Atoji, M.; Gschneidner, K., Jr.; Daane, A. H.; Rundle, R. E.; Spedding, F. H. The Structures of Lanthanum Dicarbide and Sesquicarbide by X-Ray and Neutron Diffraction. *J. Am. Chem. Soc.* **1958**, *80*, 1804−1808.

(18) Mattausch, H.; Schaloske, M. C.; Hoch, C.; Simon, A. Halogenide der Seltenerdmetalle Ln4X5Z. Teil 2: Eine orthorhombische Verknüpfungsvariante o-Ln4X5Z. *Z. Anorg. Allg. Chem.* **2008**, *634*, 498−502.

(19) Holley, C. E., Jr.; Mulford, R. N. R.; Ellinger, F. H.; Koehler, W. C.; Zachariasen, W. H. The Crystal Structure of Some Rare Earth Hydrides. *J. Phys. Chem. A* **1955**, *59*, 1226−1228.

(20) Nicol, A. T.; Vaughan, R. W. Proton chemical shift tensors of alkaline earth hydrides. *J. Chem. Phys.* **1978**, *69*, 5211−5213.

(21) Franco, F.; Baricco, M.; Chierotti, M. R.; Gobetto, R.; Nervi, C. Coupling Solid-State NMR with GIPAW ab Initio Calculations in Metal Hydrides and Borohydrides. *J. Phys. Chem. C* **2013**, *117*, 9991−9998.

(22) Kayser, F. X. Diffraction evidence for the existence of an F.C.C. ⇄ H.C.P. transformation in Yb. *Phys. Status Solidi A* **1971**, *8*, 233−241.

(23) Atoji, M.; Flowers, R. H. Neutron Diffraction Study of YbC2 at 300−2°K. *J. Chem. Phys.* **1970**, *52*, 6430−6431.

(24) Haschke, J. M.; Eick, H. A. Phase investigation of the ytterbium–carbon system. *J. Am. Chem. Soc.* **1970**, *92*, 1526−1530.

(25) Warf, J. C.; Hardcastle, K. A HIGHER HYDRIDE OF YTTERBIUM. *J. Am. Chem. Soc.* **1961**, *83*, 2206−2207.

(26) Reckeweg, O.; Lissner, F.; Schleid, T. Single Crystals of Cotunnite-Type YbH2. *Z. Anorg. Allg. Chem.* **2012**, *638*, 1595.

(27) Bowman, R. C.; Fultz, B. Metallic Hydrides I: Hydrogen Storage and Other Gas-Phase Applications. *MRS Bull.* **2002**, *27*, 688−693.

(28) Cockcroft, J. K.; Kremer, R. K.; Mattausch, H.; Raju, N. P.; Simon, A. Structure and magnetic ordering of holmium carbide fluoride, Ho2CF2. *J. Alloys Compd.* **1992**, *183*, 241−251.

(29) Pflug, C.; Rudolph, D.; Schleid, T.; Kohlmann, H. Hydrogenation reaction pathways and crystal structures of La_2H_2Se, La_2H_3Se and La_2H_4Se. *Eur. J. Inorg. Chem.* **2022**, *2022*, No. e202101095.